Talanta 127 (2014) 94–99

Contents lists available at ScienceDirect

Talanta

journal homepage: www.elsevier.com/locate/talanta

A new Methimazole sensor based on nanocomposite of CdS NPs–RGO/IL–carbon paste electrode using differential FFT continuous linear sweep voltammetry

Parviz Norouzi [a,b,*], Vinod Kumar Gupta [c,**], Bagher Larijani [d], Mohammad Reza Ganjali [a,b], Farnoush Faridbod [a,b]

[a] Center of Excellence in Electrochemistry, University of Tehran, Tehran, Iran
[b] Biosensor Research Center, Endocrinology and Metabolism Molecular-Cellular Sciences Institute, Tehran University of Medical Sciences, Tehran, Iran
[c] Department of Chemistry, Indian Institute of Technology Roorkee, Roorkee 247 667, India
[d] Diabetes Research Center, Endocrinology and Metabolism Clinical Sciences Institute, Tehran University of Medical Sciences, Tehran, Iran

ARTICLE INFO

Article history:
Received 16 February 2014
Received in revised form
22 March 2014
Accepted 25 March 2014
Available online 1 April 2014

Keywords:
Differential FFT continuous linear sweep voltammetry
Methimazole
Reduced graphene oxide
CdS nanoparticles
Ionic liquid

ABSTRACT

A Methimazole sensor was designed and constructed based on nanocomposite of carbon, ionic liquid, reduced graphene oxide (RGO) and CdS nanoparticles. The sensor signal was obtained by Differential FFT continuous linear sweep voltammetry (DFFTCLSV) technique. The potential waveform contains two sections, preconcentration potential and potential ramp. In this detection technique, after subtracting the background current from noise, the electrode response was calculated, based on partial and total charge exchanges at the electrode surface. The combination of RGO and CdS nanoparticles can catalyze the electron transfer, which outcomes of the amplification of the sensor signal. The result showed that the sensor response was proportional to the concentrations of Methimazole in the range of 2.0 to 300 nM, with a detection limit of 5.5×10^{-10} M. The sensor showed good reproducibility, long-term of usage stability and accuracy. The characterization of the sensor surface was studied by atomic force Microscopy and Electrochemical Impedance Spectroscopy. Moreover, the proposed sensor exhibited good accuracy, and R.S.D value of 2.82%, and the response time of less than 7 s.

1. Introduction

Methimazole (2-mercapto-1-methylimidazole) (Fig. 1) used in treatment of hyperthyroid by the production of thyroxin, a hormone excreted by the thyroid gland, inhibits the formation of thyroid hormones [1]. It is absorbed by the gastrointestinal tract and acts as an immunosuppressive agent in Graves' disease [2–5]. Methimazole may cause side effects such as irritation of the skin, allergies, pharyngitis with fever, nephritis, liver cirrhosis, impaired taste, olfactory and auditory [6]. Therefore, it is required to develop a rapid and sensitive technique for determination of Methimazole in clinical chemistry, nutrition and pharmaceutical formulations. Numerous analytical procedures have been reported for determination of Methimazole including spectroscopy [7,8], gas chromatography–mass spectrometry (GC–MS) [9,10], high-performance liquid chromatography–mass spectrometry (HPLC–MS) [11], flow-injection [12] and capillary electrophoresis [13].

It is well known that nanostructures of carbon, like reduced graphene oxide (RGO) demonstrate high surface area beside suitable electrical conductivity in new designed electrodes; also, it helps to establish a larger number of active sites for adsorption of organic molecules [14–17]. Those excellent characterizations of RGO can facilitate the electron transfer of electroactive species. Moreover, in order to improve the performance of the carbon paste electrode, ionic liquids (IL) can be very helpful as a binder in the carbon paste electrodes [18]. Here, IL was used as a binder in the nanocomposite electrode to its high ionic conductivity, good stability and well biocompatibility. Also, IL, mixed with CdS nanoparticles (CdS NPs) that arrested onto RGO paste electrodes, exhibited direct electrochemistry, and catalytic activity towards oxidation of compounds. Also, it was noted that CdS NPs were used to incorporate with enzyme for realizing the direct electron transfer, and CdS has been found efficiently enhancing the electron transfer reactivity of the electrode surface [19,20]. It has been reported that the integration of RGO and CdS NPs offer synergy effects in electrocatalytic applications, so we have reasons to expect the nanocomposite of RGO and CdS NPs has

* Corresponding author at: Center of Excellence in Electrochemistry, University of Tehran, Tehran, Iran. Tel.: +98 21 61112294.
** Corresponding author.
E-mail addresses: norouzi@khayam.ut.ac.ir (P. Norouzi), vinodfcy@gmail.com (V.K. Gupta).

http://dx.doi.org/10.1016/j.talanta.2014.03.061
0039-9140/

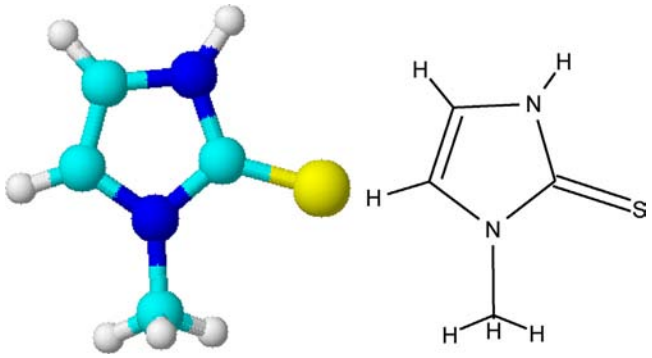

Fig. 1. Chemical structure of Methimazole.

the same effect, which has not been reported as the best of our knowledge.

The main objective of this work is the first application of differential fast Fourier transform continuous linear sweep voltammetry (DFFTCLSV) technique to develop a new sensor for the trace determination of Methimazole. It was used to investigate the electrochemical response of Methimazole on the surface of composite carbon paste electrode. The composite was a mixture of IL, CdS NPs and RGO, which develop a novel electrochemical sensor that provides a situation for improving electrocatalytic activities for electrochemical detection of Methimazole. In fact, at the optimal conditions, the electrode response was integrated currents in the potential range of the analyte peak in form of coulomb. The sensor response was proportional to Methimazole concentration. The sensor surface was characterized by atomic force microscopic (AFM) and electrochemical impedance spectroscopy (EIS) techniques.

2. Materials and methods

2.1. Reagents

All chemicals and solvents used were of analytical grade and were used as received. 1-Butyl-3-methylimidazolium hexafluorophosphate ([BMIM][PF_6], IL), were purchased from Merck Company (Germany). Methimazole was purchased from Sigma-Aldrich, and stored frozen. CdS nanoparticles were prepared according to Ref. [19]. The solution 3 mM $Fe(CN)_6^{4-}/^{3-}$ in 0.1 M KCl. The standard solutions were prepared with double distilled water when in use, except as otherwise stated. Double distilled water was used throughout the experiment.

2.2. The sensor fabrication

At first, the modified carbon paste electrode (CILE) was prepared by hand-mixing of 10 g of graphite powder and 4 g of IL ([BMIM][PF_6]). They were mixed thoroughly in a mortar and heated at a temperature of 60 °C to form a homogeneous carbon paste. The paste was packed into a cavity of a glass tube (i.d. 4 mm). An electrical contact was established via a copper wire to the paste in the inner hole of the tube. The carbon–IL paste electrode (CILE) was fabricated with the mentioned procedure. It was then left to cool at room temperature. A mirror-like surface was obtained by smoothing the electrode on the weighing paper.

Primarily, GO was prepared by a modified Hummers technique using expandable graphite flakes as the original material [21]. Expandable graphite flakes (1 g) were triturated with NaCl (45 mg/mL) for 15 min, and subsequently NaCl was dissolved in water and removed by filtration. The RGO was then prepared by a chemical reduction of the 0.6 mg/mL GO powder in distilled water with 160 mM $NaBH_4$). The mixture was kept at 90 °C for 30 min. The product was centrifuged to precipitate the RGO powder, which was eventually dried in vacuum at low temperature. Then, 50–400 μL of 4.0 mg/mL RGO and 10–80 μL of 5 g/L CdS NPs suspension solution were mixed together, diluted to 1.0 mL with 0.1 M PBS (pH 6.5), and sonicated homogeneously. Then 8.0 μL of the mixture was cast onto the newly prepared CILE surface and left it to dry at room temperature. The resulted electrode was denoted as RGO–CdS NPs/CILE. The sensor was rinsed throughout with doubly distilled water. When not in use, the fabricated electrode was stored in pH 5.0 PBS at 4 °C in a refrigerator. The sensor was rinsed throughout with doubly distilled water. The electrochemical experiments were performed in a solution of 0.1 M acetate buffer containing 20 mM NaCl (ABS, pH 6.5).

2.3. Apparatus

Atomic force microscopic (AFM) images were obtained by using Agilent instrument with non-contact mode was used while mapping the surface. The electrochemical DFFTCLSV was carried out with a homemade potentiostat [22–35] was connected to a PC equipped with an analog to digital data acquisition board (PCL-818H, Advantech Co.). Electrochemical cell was a conventional three-electrode system with a working electrode, a platinum wire as an auxiliary electrode and a saturated calomel electrode (SCE) as the reference electrode. The condition for the data acquisition requirements, electrochemical software was developed using Delphi 6.0. The program was used to generate an analog waveform and acquire current readings [22–35]. The potential waveform consists of two parts; (a) Potential steps, where accumulation of analyte takes place (−100 mV striping potential was applied for 0.5 s); (b) the final part, potential ramp, in which current measurements take place. The potential waveform was repeatedly applied to the working electrode and then the data was acquired, and stored by the software. Also, the program was able to process and plot the data in real time. EIS measurements were performed in 3 mM $K_3Fe(CN)_6$ in 0.1 M KCl. A stock solution of 2 mM of Methimazole was firstly prepared, and then an aliquot was diluted to the appropriate concentration.

3. Results and discussion

In order to study the surface of RGO–CdS NPs/CILE was examined by AFM. This technique was employed to investigate the surface topography of prepared composite film. The topographic features visible on different length scales allowed the relocation of an identical scan area after the CdS NPs dispersion. Fig. 2 shows surface topography image of RGO–CdS NPs/CILE thin composite film. As shown in the figure, the RGO–CdS NPs/CILE formed was in the range of nanometers, which result in a large surface area and easier attachment of the film. As shown, the samples of CdS NPs dispersion stabilized by IL and RGO, and reveals that the thickness of formed composite is more than 50 nm, where it seems the size of NPs was 5–30 nm. Also, in this image, it can be seen that the CdS NPs were dispersed among RGO. Formation of RGO layer on the surface of CILE is necessary to reach a sufficient thickness to create a satirically a good porosity and stabilized CdS NPs on the surface. EIS technique is a successful instrument to study the structures formation of the sensor. Fig. 3 demonstrates EIS curves for the unmodified CILE, RGO/CILE and RGO–CdS NPs/CILE in 0.1 M KCl solution containing 3 mM $K_3Fe(CN)_6/K_4Fe(CN)_6$, respectively.

The results suggested that the R_{ct} (charge transfer impedance) of RGO/CILE (curve *b*) was lower than that was obtained for the bare CILE electrode. This could be of a higher collection of $K_3Fe(CN)_6/K_4Fe(CN)_6$ on the sensor surface. Also, the value of Z for

RGO–CdS NPs/CILE (curve *c*) is also, lower than that of the unmodified CILE, proposing that the smaller of CdS NPs coat on the sensor surface, which is an indication of the better conductivity of RGO–CdS NPs/CILE.

Fig. 4 illustrated the linear sweep voltammograms of Methimazole on RGO–CdS NPs/CILE in ABS, pH 6.5. The curves (in range of −100 to 900 mV/s) show a well-defined oxidation peak on the modified electrode, in which anodic peak potentials is about 650 mV. The modification could enhance the value of the electron-transfer rate, and may also provide conditions for higher accumulation capacity and catalytic ability of the sensor surface to contribute in the oxidation reaction of Methimazole [36]. Fig. 4B demonstrates the measured current peaks of 2 μM Methimazole in AB solution at pH 6.5 vs. root of scan rates. The peak current was grown in the scan rates in the range from 5 to 2000 mV/s, and there is a fine linear relationship between the peak current and root of scan rate, with equations as $i_p = 155.82\,\nu^{1/2} + 2.4541$ ($R^2 = 0.993$). These results, suggest that the reaction is diffusion-controlled electron transfer process.

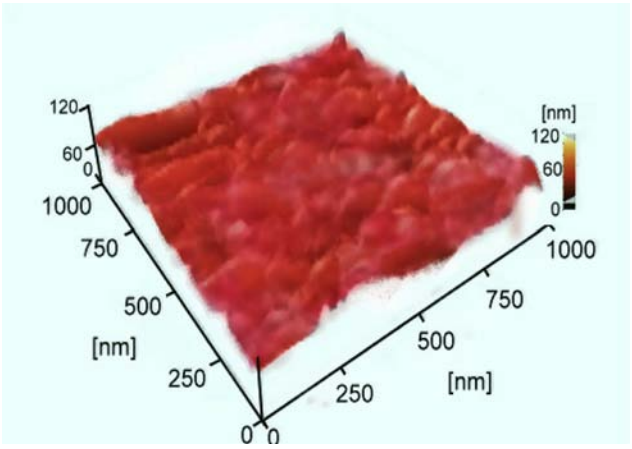

Fig. 2. AFM images of RGO–CdS NPs/CILE.

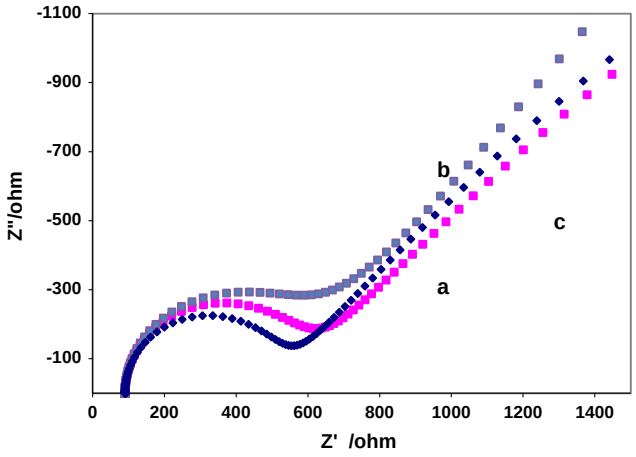

Fig. 3. EIS plots of the modified electrode in 3 mM $K_3Fe(CN)_6$ with 0.1 M KCl: (a) bare CILE (b) RGO/CILE and (c) RGO–CdS NPs/CILE.

3.1. Analytical procedure and determination of the sensor response

A stock solution of 5 mM Methimazole was prepared, and then an aliquot was diluted to the required concentration. For measurement, the three-electrode system was installed in AB solution at pH 6.5. In this technique, all the currents in DFFTCLS voltammograms were subtracted from the voltammograms that were recorded in absent of Methimazole,

$$\Delta I = i - i_0 \tag{1}$$

where, i is current of the recorded cyclic voltammogram, and i_0 represents i, in the absence of the adsorbent of the analyte. In DFFTCLSV technique charge (Q) passing through the sensor was calculated during the potential ramp.

Fig. 5 illustrates the recorded DFFTCLS voltammograms of the sensor in potential range −100 to 900 mV and in time window (180 s), to addition of 5.0×10^{-7} M Methimazole. In this graph, the time axis represents the time of experiment was running. The potential axis on this graph represents potential range that applied to the working electrode during each potential ramp. The figure shows that after addition of Methimazole in AB solution at pH 6.5, a signal appears at potential 650 mV. As mentioned above the excessive accumulation of the analyte on the surface of the sensor could improve of direct electron transfer between the active sites and Methimazole molecules.

The sensor response (in form of ΔQ) was calculated based on the integration of the current changes in a selected potential range at the recorded DFFTCLS voltammograms.

$$\Delta Q_n = Q_n - Q_0 = \Delta t \left[\sum_{E=E_i}^{E=E_f} |i(n,E) - i(n_0,E)| \right] \tag{2}$$

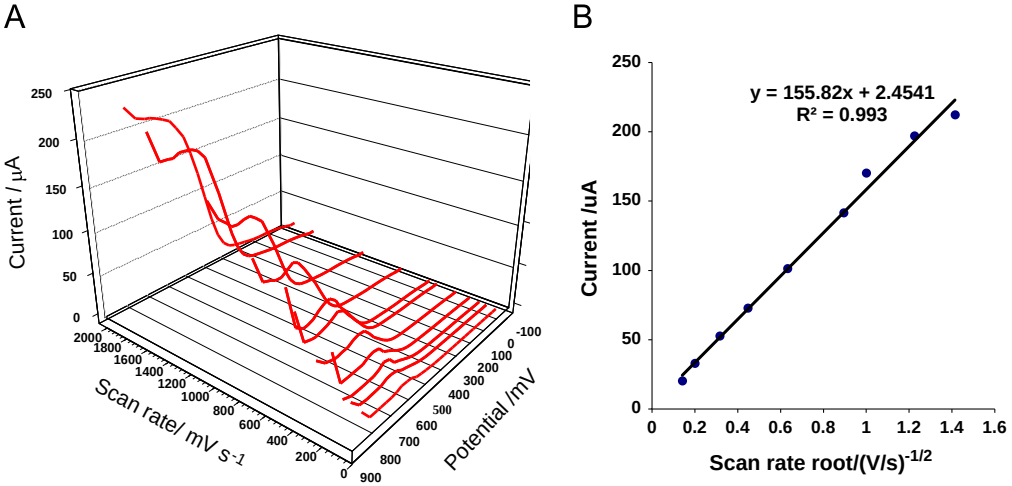

Fig. 4. (A) Typical linear sweep voltammograms of 2 μM Methimazole in AB solution at pH 6.5, RGO–CdS NPs/CILE; scan rates 5 to 2000 mV/s, (B) the measured current peaks vs root of scan rates.

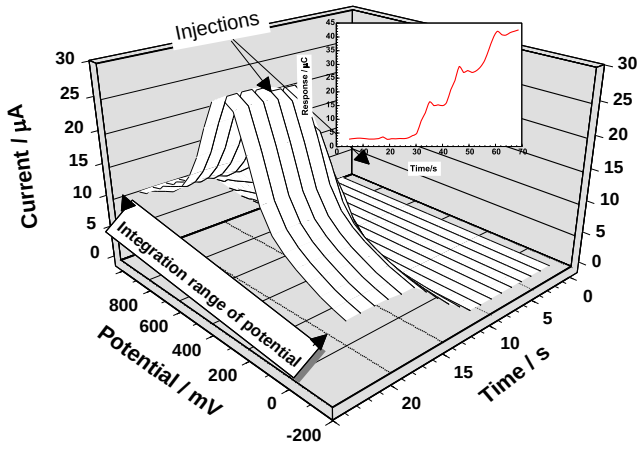

Fig. 5. DFFTCLS voltammograms of the RGO–CdS NPs/CILE; in absent and present of 5.0×10^{-7} M Methimazole in AB solution at pH 6.5, in the potential range of −100 to 900 mV at potential scan rate 1600 mV/s. The inset integrated response of the sensor.

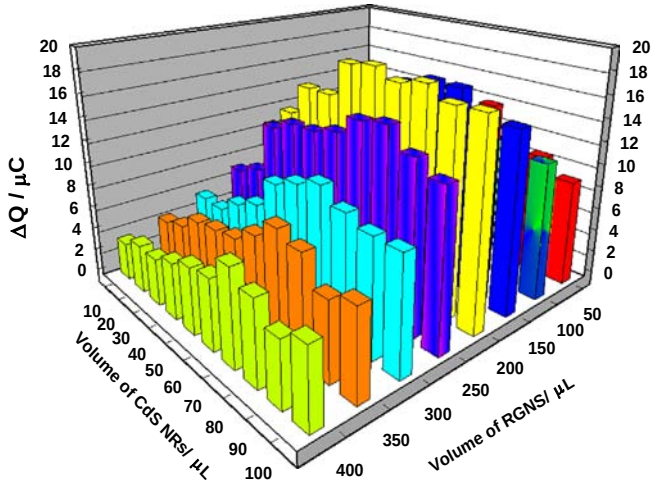

Fig. 6. The effect of amount of CdS and RGO on the sensor response to 3.0×10^{-7} M of Methimazole in AB solution at pH 6.5. In the potential range of −100 to 900 mV at potential scan rate 1600 mV/s.

where, n is number of scan ($n>0$), Q_n is the electrical charge obtained by integration of n^{th} LS voltammogram curve between −100 and 900 mV, and Q_0 represents the value of Q in the absence of the analyte (see the inset graph in Fig. 5). Furthermore, the results indicate that with increasing the concentration of Methimazole the spiked standard sample solution ΔQ increases proportionally. By optimizing the most important parameters in the detection system, it is possible to improve the S/N Methimazole response to obtain maximum sensitivity.

3.2. The effect of nanoparticles amount in the sensor fabrication

Fig. 6 shows the effect amount of CdS NPs and RGO on the sensor response to 3.0×10^{-7} M Methimazole in AB solution at pH 6.5. Where, different volumes of solutions 4.0 mg/mL RGO and 5 g/L CdS nanoparticles suspension solution was casted on the electrode surface. In the ingratiation potential range, for calculating the response of sensor was −100 to 900 mV at potential scan rate 1600 mV/s.

The figure demonstrates that the change of the sensor response with the amount of RGO and CdS NPs in the content of the modifier or film composition. In these measurements, various volumes of solution RGO (50 to 400 μL) and CdS (10 to 100 μL) in constant volume of IL were tested. The graph indicates that the value of ΔQ increases with the increasing of RGO up to 200 μL and then decreases slightly. Moreover, as shown in figure, for CdS NPs the value of ΔQ increase with the volume of the CdS in the sensor composition up to 70 μL. Though, at the higher volume of CdS NPs, the value of ΔQ decreases. This could be due to the increase of the resistance of the surface electrode at more CdS NPs. It was seen that in absent of the NPs there is no significant redox peak current in the voltammogram. In addition, the results presented in the figure indicate creating a high surface area, conductivity and catalytic effect of increase sensitivity of detection technique.

3.3. Optimization of pH

The pH effect on the sensor performance was investigated by measuring the electrode response to 2.0×10^{-7} M Methimazole in various pHs. The pH was changed at a definite range in order to determine the optimum value, in which the sensitivity of the sensor is the highest. As shown in Fig. 1, the structure of Methimazole contains NH groups, which measurement could be the influenced by the pH of solution. Due to this reason determination of the optimum pH is one of the important parameter in solution. Fig. 7 shows the results of examination of pH on the detection technique sensitivity. The DFFTCLSV measurements were recorded at scan rate of 1600 mV/s. The sensor response increases gradually from pH 4.0 to 8.0 and after achieving the maximum, the response decreases, indicating that the optimum pH 6.5 can be used for the detection of Methimazole.

3.4. Optimization of scan rate

Due to this fact that the response of the detector is diffusion controlled, it can be expected that the sensitivity of the measurements to be depend on the potential scan rate. So, the influence of scan rates on the sensitivity of the detector response to addition of solutions having a concentration of 2.0×10^{-7} M of Methimazole was investigated, at scan rates 100 to 2000 mV/s). As shown in the Fig. 8, the detector exhibits the maximum sensitivity at 1600 mV/s of scan rate. The effects of the sweep rate on the detection performance can be taken into consideration from different aspects, such as the speed in data acquisition during the current sampling, which may due to limitation in analog-to-digital broad, second and limitations in kinetic factors of rate of electrochemical processes.

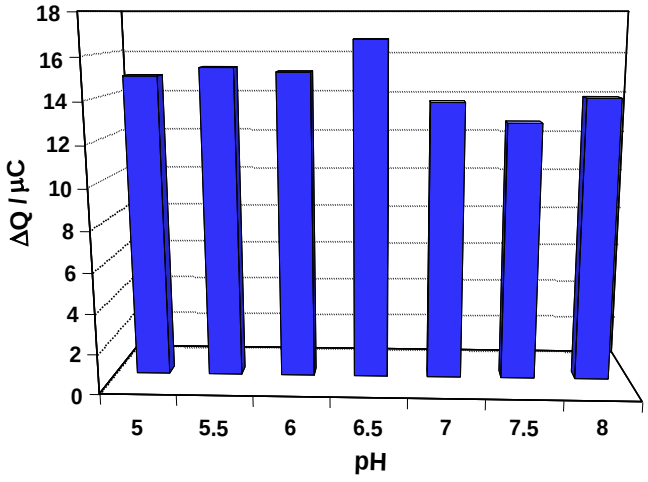

Fig. 7. The effect of pH concentration on the sensor response to 2.0×10^{-7} M in AB solution at pH 6.5, in the potential range of −100 to 900 mV at potential scan rate 1600 mV/s.

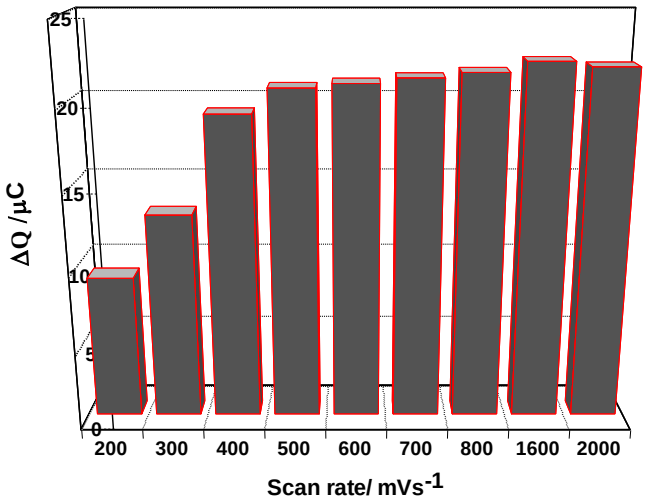

Fig. 8. The effect of the scan rate on the response of RGO–CdS NPs/CILE in 2.0×10^{-7} M Methimazole in AB solution at pH 6.5, in the potential range of −100 to 900 mV.

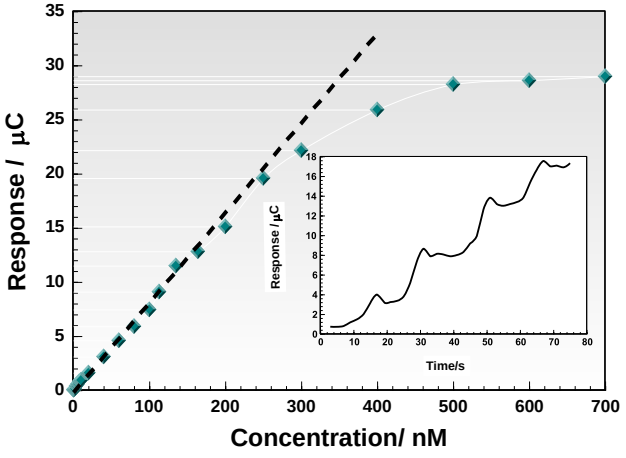

Fig. 9. Response (ΔQ) of the RGO–CdS NPs/CILE to Methimazole upon the following concentrations: (A) 2 to 700 nM in AB solution at pH 6.5, in the potential range of −100 to 900 mV at potential scan rate 1600 mV/s., (B) The inset is curve response for addition of 20 nM Methimazole solution.

3.5. Calibration curve

Under optimal conditions in the determination of the presence of Methimazole, the response time, which is defined as the time when 95.7% of the steady-state response is reached at about 7 s with DFFTCLSV technique. Fig. 9 illustrates a typical ΔQ response of the RGO–CdS NPs/CILE to a set of standard solutions of Methimazole (from 2.0 to 200.0 nM in 1.0×10^{-3} M in AB solution at pH 6.5, in the potential range of −100 to 900 mV at potential scan rate 1600 mV/s. In this figure, each point represents the integrated signal for 3 consecutive additions of the Methimazole standard solutions.

In general, the inset figure shows the analyte response has a linear dynamic range of 2 to 300 nM, with correlation coefficient of $R^2=0.992$ values. The estimated detection limit based on signal to noise ratio ($S/N=3$), was found 5.5×10^{-10} M. A long-term storage stability of the RGO–CdS NPs/CILE was tested for 70 days, and it was seen that the sensitivity retained 96.8%.

The performances of the electrochemical technique is compared with some of the best previously reported Methimazole measurement [37,38] based on the utilization of different materials as the sensor and different detection techniques (Table 1) and it was confirmed that the presented RGO–CdS NPs/CILE sensor with DFFTCLSV exhibited an excellent and reproducible sensitivity.

Table 1
The comparison of the proposed sensor with the best previous reported ones based on the utilization of different materials.

Ref.	Detection technique	DL	The electrode
37	Cyclic voltammetry (CV), differential pulse voltammetry	2.0×10^{-8} M	Enhanced electrochemical response of Methimazole at the acetylene black/chitosan composite film modified glassy carbon electrode
38	Voltammetry	9.36×10^{-9} M	Based on the modification of a glassy carbon electrode with multi-walled carbon nanotube/electro-copolymerized cobalt nanoparticles-poly(pivalic acid) composite
This work	FFTCLSV	6.5×10^{-10} M	RGO–CdS NPs/CILE

4. Conclusions

RGO–CdS NPs/CILE nanocomposite sensor can provide a unique microenvironment for the direct electrochemistry of Methimazole. Also, application of DFFTCLSV technique provides a novel coulometric determination of Methimazole, which is highly sensitive. Such sensitivity is attributed to the synergy effect of RGO and CdS NPs on the oxidation of Methimazole. It can be suggested that the sensor has excellent responses because of the large surface area and fast electron transfer of graphene nanoparticles. Using DFFTCLSV technique creates reproducible signals with response time less than 9 s and detection limit of 5.5×10^{-10} M. In addition, the electrochemical technique reveals some other excellent characteristics such as wide linear range, low detection limit and relatively a long-term stability for 70 days. Also the proposed sensor has easy fabrication and low cost. All these characteristics suggest that the new strategy for using RGO–CdS NPs nanocomposites sensor and DFFTCLSV technique is good for determination of such molecules.

Acknowledgements

The authors are grateful to the Research Council of University of Tehran (Grant no. 6102027) for the financial support of this work.

References

[1] M. Aletrari, P. Kanari, D. Partassides, E. Loizou, J. Pharm. Biomed. Anal. 16 (1998) 785–792.
[2] Antithyroid agents, Martindale, in: J.E.F. Reynolds (Ed.), The Extra Pharmacopoeia, 29th ed,The Pharmaceutical Press, London, 682–688.
[3] H.Y. Aboul-Enein, A.A. Methimazol Al-Badr, in: K. Forey (Ed.), Analytical Profiles of Drug Substance, 18, Academic Press, New York, 1979, pp. 351–371.
[4] A.P. Weetman, A.M. McGregor, R. Hall, Clin. Endocrinol. 21 (1984) 163–172.
[5] P. Kendall-Taylor, Br. Med. J. 288 (1984) 509–511.
[6] A.C. Edward, Thyroid hormones and drugs that affect the thyroid, in: C.M. Smith, A.M. Reynard (Eds.), Text-Book of Pharmacology, W.B. Saunders Company, Philadelphia, PA, 1992, pp. 652–656.
[7] C. Sanchezpedreno, M.I. Albero, M.S. Garcia, V. Rodenas, Anal. Chim. Acta 308 (1995) 457–461.
[8] M.S. Garcia, M.I. Albero, C. Sanchezpedreno, L. Tobal, Analyst 120 (1995) 129–133.
[9] Q.H. Zou, Y. Liu, M.X. Xie, J. Han, L. Zhang, Anal. Chim. Acta 551 (2005) 184–191.

[10] L. Zhang, Y. Liu, M.X. Xie, Y.M. Qiu, J. Chromatogr. A 1074 (2005) 1–7.
[11] K. De Wasch, H.F. De Brabander, S. Impens, M. Vandewiele, D. Courtheyn, J. Chromatogr. A 912 (2001) 311–317.
[12] L. Hollosi, A. Kettrup, K.W. Schramm, J. Pharm. Biomed. 36 (2004) 921–924.
[13] A. Wang, L. Zhang, S. Zhang, Y. Fang, J. Pharm. Biomed. Anal. 23 (2000) 429–436.
[14] S.A. Zaidi., Int. J. Electrochem. Sci. 8 (2013) 11337–11355.
[15] S. Wu, Q. He, C. Tan, Y. Wang, H. Zhang, Small 9 (2013) 1160–1172.
[16] C. Punckt, M.A. Pope, J. Liu, Y. Lin, I.A. Aksay, Electroanalysis 22 (2010) 1027–1036.
[17] D.A.C. Brownson, D.K. Kampouris, C.E. Banks, Chem. Soc. Rev. 41 (2012) (6944-697).
[18] F. Faridbod, M.R. Ganjali, P. Norouzi, S. Riahi, H. Rashedi, Application of Ionic Liquids in Electrochemical Sensors and Biosensors as a Chapter in the Book Entitled: "Ionic Liquids, Theory and Applications", INTECH Publisher, 2011 (Chapter, 9).
[19] Y. Huang, W. Zhang, H. Xiao, G. Li, Biosens. Bioelectron. 21 (2005) 817–821.
[20] X.Y. Dong, X.N. Mi, W.W. Zhao, J.J. Xu, H.Y. Chen, Biosens. Bioelectron. 26 (2011) 3654–3659.
[21] W.S. Hummers, R.E. Offeman, J. Am. Chem. Soc. 80 (1958) (1339-1339).
[22] P. Norouzi, M.R. Ganjali, B. Larijani, A. Mirabi-Semnakolaii, F.S. Mirnaghi, A. Mohammadi, Pharmazie 63 (2008) 633–637.
[23] P. Norouzi, M.R. Ganjali, S. Shirvani-Arani, A. Mohammadi, J. Pharm. Sci. 95 (2007) 893–904.
[24] M.R. Pourjavid, P. Norouzi, M.R. Ganjali, Int. J. Electrochem. Sci. 4 (2009) 923–942.
[25] P. Norouzi, M.R. Ganjali, M. Zare, A. Mohammadi, J. Pharm. Sci. 96 (2007) 2009–2017.
[26] P. Norouzi, M. Qomi, A. Nemati, M.R. Ganjali, Int. J. Electrochem. Sci. 4 (2009) 1248–1261.
[27] P. Norouzi, B. Larijani, M. Ezoddin, M.R. Ganjali, Mater. Sci. Eng., C 28 (2008) 87.
[28] M.R. Ganjali, P. Norouzi, R. Dinarvand, R. Farrokhi, A.A. Moosavi-Movahedi, Mater. Sci. Eng., C 28 (2008) 1311–1318.
[29] P. Norouzi, M.R. Ganjali, L. Hajiaghababaei, Anal. Lett. 39 (2006) 1941–1953.
[30] P. Norouzi, G.R. Nabi Bidhendi, M.R. Ganjali, A. Sepehri, M. Ghorbani, Microchim. Acta 152 (2005) 123–129.
[31] P. Norouzi, M.R. Ganjali, T. Alizadeh, P. Daneshgar, Electroanalysis 18 (2006) 947–954.
[32] M.R. Ganjali, P. Norouzi, M. Ghorbani, A. Sepehri, Talanta 66 (2005) 1225–1233.
[33] P. Norouzi, H. Ganjali, B. Larijani, F. Faridod, M.R. Ganjali, H.A. Zamani, Int. J. Electrochem. Sci. 6 (2011) 5189–5199.
[34] P. Norouzi, B. Larijani, F. Faridbod, M.R. Ganjali, Int. J. Electrochem. Sci. 5 (2010) 1550–1562.
[35] P. Norouzi, M.R. Ganjali, M. Qomi, A.N. Kharat, H.A. Zamani, Chin. J. Chem. 28 (2010) 1133–1139.
[36] K. Wang, Q. Liua, L. Daia, J. Yana, C. Jua, B. Qiua, X. Wua, Anal. Chim. Acta 695 (2011) 84–88.
[37] W. Yazhen, Bioelectrochemistry 81 (2011) 86–90.
[38] A. Kutluay, M. Aslanoglu, Sens. Actuators, B 171-172 (2012) 1216–1221.